

# Virtual source approach to scattering from partially buried elastic targets

Henrik Schmidt

*Department of Ocean Engineering, Massachusetts Institute of Technology, Cambridge, MA 02139*

**Abstract.** A hybrid modeling framework for scattering from general 3D elastic targets in a stratified ocean waveguide is presented, incorporating multiple scattering between the target and the stratification, and allowing for targets to be completely or partially buried in a stratified seabed. The approach uses a generalized wavefield superposition, or virtual source approach, together with a Fourier-Bessel spectral representation of the Green's function in a stratified ocean, to model scattering from targets described solely by their arbitrary surface geometry and dynamic stiffness. The hybrid approach is here implemented within the OASES-3D modeling framework, with the target surface stiffness determined either analytically, or numerically using Finite Elements.

## INTRODUCTION

A hybrid modeling framework for scattering from completely proud or buried targets has been developed and used extensively in the analysis of experimental data collected during the GOATS'98, '2000, and '2002 experiments carried out jointly by MIT and SACLANTCEN [1, 2, 3]. It uses OASES to compute the incident field at the target position, anywhere in a stratified fluid-elastic waveguide. This field is then convolved with the free-field scattering function for elastic targets such as spherical shells, effectively replacing the target by a virtual, multipole source at the target position, the 3D radiation from which is directly computed using OASES-3D [4].

This single-scattering approach ignores all multiple interactions between the target and the seabed, and is incapable of treating partially buried targets. To more realistically represent the shallow water mine-countermeasures problem, the OASES-3D target modeling framework is being combined with a high-fidelity Finite Element modeling framework, FESTA [5, 6], developed at SACLANTCEN, to form a new hybrid modeling capability for completely or partially buried targets, incorporating seabed interference. The coupling is achieved by representing the scattered field by a superposition of fields produced by a virtual source distribution within the target surface, including their seabed interaction.

The virtual source field is superimposed with the incident field, and the virtual source strengths are determined from the known boundary conditions on the surface of the target. The boundary conditions for any elastic target may be expressed in terms of the dynamic stiffness matrix, expressing the unique relation between the surface pressure and the normal displacements. The stiffness matrices, which are independent of the surrounding medium, may be computed by any independent, suitable method, e.g. using finite elements for complex targets, or Green's theorem for homogeneous targets.

The scattered field in the waveguide is then computed using the 'exact' multipole expansion of point source distributions inherent in OASES-3D. As opposed to other coupling approaches such as the 'scattering chamber' approach, this virtual source approach does not require the treatment of the outer medium by the target model. Thus, once the dynamic stiffness matrix for the target is determined, e.g. in-vacuo or submerged in a homogeneous medium, it can be used for arbitrary orientation and burial of the target. This approach is therefore convenient for investigating sensitivity of the scattering to seabed properties, burial depth, insonification geometry, etc.

The present virtual source approach may be considered a full 3D generalization of the so-called internal source density method which has been applied in the past to model the scattering from targets of simple geometry or boundary conditions. For example, it has been used by Stepanishen [7] to model 3D scattering from objects of revolution with ideal Dirichlet or Neumann boundary conditions. However, in addition to the homogeneous boundary conditions and the axisymmetric target geometry, it was assumed that the outer medium be an infinite, homogeneous fluid, as has been the case in most other applications as well. As an exception, Kessel used a similar internal multipole expansion method in combination with a modal Green's function to model the scattering from objects in horizontally stratified waveguides, again assuming ideal, homogeneous boundary conditions [8]. Also, that approach does not allow the target to penetrate the waveguide interfaces, and does not incorporate multiple scattering between the target and the adjacent boundaries.

In contrast to such earlier work, the present approach applies to general elastic objects with full 3D geometry, with all required being a frequency-dependent stiffness matrix, uniquely associated with the internal structure and composition. Also, the present approach allows the target to be penetrating any interface in a horizontally stratified ocean environment, thus providing a versatile numerical method for analysis of scattering from partially and completely buried targets, incorporating multiple scattering effects, within the targets as well as between the target and the environmental stratification.

The dynamic stiffness matrix for the target may be modeled using any applicable approach. Thus, for a homogeneous fluid object it may be determined using a 'reverse' virtual source approach, while for a spherical shell it may be computed using an exact spherical harmonics representation, or using a more general numerical method such as Finite Elements.

## **THEORY**

### **Virtual Source Approach**

The virtual source approach is fundamentally a wavefield superposition approach, replacing the target by a distribution of acoustic sources placed in the background medium, inside the surface of the target, and of unknown magnitude and phase. These virtual source strengths are then found from the condition that the superposition of their generated field with the incident field on the surface of the volume occupied by the target must satisfy the boundary conditions associated with the true target.

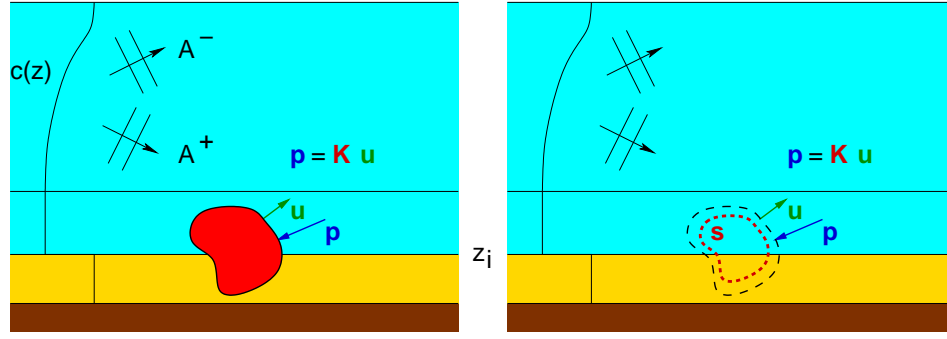


**FIGURE 1.** Partially buried target in stratified ocean waveguide. (a) Elastic target partially buried in seabed. (b) Target replaced by internal, virtual source distribution generating field which superimposed with incident field satisfies boundary condition prescribed by the target characteristics.

This simple superposition principle is illustrated schematically in Fig. 1. The plot to the left shows an arbitrarily shaped object in a stratified ocean, here partially buried in the seabed at depth  $z_i$ . The stratification can include fluid as well as elastic layers, but it is here for simplicity assumed that the layers containing the target are isovelocity fluid media. In the plot to the right, the target is removed and replaced by a continuously stratified medium with a discrete distribution of  $N$  simple point sources, the unknown, complex strengths of which are represented by the vector  $\mathbf{s}$ . This source distribution is assumed to generate a field which is identical to the scattering produced by the target.

If the surface of the target is discretized in  $N$  nodes, the total pressure  $\mathbf{p}$  and normal displacement  $\mathbf{u}$  at the nodes are decomposed into the known incident field contribution  $\mathbf{p}_i, \mathbf{u}_i$ , and the scattered field,  $\mathbf{p}_s, \mathbf{u}_s$ ,

$$\mathbf{p} = \mathbf{p}_i + \mathbf{p}_s \quad (1)$$

$$\mathbf{u} = \mathbf{u}_i + \mathbf{u}_s, \quad (2)$$

The scattered field is generated by the virtual source distribution  $\mathbf{s}$ ,

$$\mathbf{p}_s = \mathbf{P}\mathbf{s} \quad (3)$$

$$\mathbf{u}_s = \mathbf{U}\mathbf{s} \quad (4)$$

with  $\mathbf{P}$  and  $\mathbf{U}$  being  $N \times N$  matrices containing the the pressure- and normal displacement Green's functions, respectively, between the  $N$  virtual sources and the  $N$  surface nodes.

The total field on the virtual target surface must now satisfy the boundary conditions associated with the real target. Thus, the field inside the true target must satisfy Green's theorem, providing a unique relation between the pressure and normal displacements on the surface. In a discrete representation with  $N$  surface nodes, this relation can be expressed in terms of a frequency-dependent, dynamic stiffness matrix  $\mathbf{K}$ ,

$$\mathbf{p} = \mathbf{K}\mathbf{u} \quad (5)$$

Combining Eqs. (1)-(5) then leads to the following matrix representation for the virtual source strengths.

$$\mathbf{s} = [\mathbf{P} - \mathbf{K}\mathbf{U}]^{-1}[\mathbf{K}\mathbf{u}_i - \mathbf{p}_i] \quad (6)$$

The scattered field now follows anywhere in the external medium by superposition, using the Green's function for the continuous medium, in this case the stratified ocean waveguide.

## Fourier-Bessel Green's Function

The Green's function for a stratified ocean needed for the scattered waveguide field may be computed using any of the established approaches, wavenumber integration, normal modes, or the parabolic equation [9]. However, the Green's functions in Eq. (6) are to be evaluated in the near field, ignored by the standard approaches, which also assume the source to be at the origin. However, the Fourier-Bessel wavenumber integration formulation [4] for stratified waveguides overcomes both of these complications. Thus, the field produced by a horizontal distribution of sources can be expressed in an azimuthal Fourier series of the displacement potential  $\phi(r, \theta, z)$ ,

$$\phi(r, \theta, z) = \phi_S + \phi_H = \sum_{m=0}^{\infty} [\phi_S^m(r, z) + \phi_H^m(r, z)] \begin{Bmatrix} \cos m\theta \\ \sin m\theta \end{Bmatrix}, \quad (7)$$

where  $\phi_S^m(r, z)$  and  $\phi_H^m(r, z)$  are the Fourier coefficients for the direct source contribution and the field produced by the boundary interactions, respectively. Both components are represented in terms of horizontal wavenumber integrals,

$$\begin{aligned} \phi_S^m(r, \theta, z) &= \frac{\varepsilon_m}{4\pi} \int_0^{\infty} \left[ \sum_{j=1}^N S_j \begin{Bmatrix} \cos m\theta_j \\ \sin m\theta_j \end{Bmatrix} J_m(k_r r_j) \frac{\exp jk_r |z - z_j|}{jk_z} \right] k_r J_m(k_r r) dk_r, \quad (8) \\ \phi_H^m(r, \theta, z) &= \int_0^{\infty} \left[ A_m^+(k_r) e^{jk_z z} + A_m^-(k_r) e^{-jk_z z} \right] k_r J_m(k_r r) dk_r \quad (9) \end{aligned}$$

where  $k_r, k_z$  are the horizontal and vertical wavenumbers,  $S_j$  is the complex source strength of source  $j$  at  $(r_j, \theta_j, z_j)$ , and  $A_m^+(k_r)$  and  $A_m^-(k_r)$  are the complex azimuthal Fourier coefficients of the up- and downgoing wavefield amplitudes produced by the multiple boundary interactions. They are found by matching the boundary conditions at all horizontal interfaces.  $\varepsilon_m$  is a factor which is 1 for  $m = 0$ , and 2 otherwise.

In the present implementation we apply the full Direct Global Matrix [9] implementation of OASES-3D for evaluating Eq. (8)-(9). However, for the Green's functions needed for Eq. (6) we will only consider interactions with the target interface  $z_i$ , allowing the amplitudes  $A_m^+$  and  $A_m^-$  in Eq. (9) to be expressed explicitly in terms of the plane wave reflection and transmission coefficients associated with this interface. This approximation therefore ignores multiple interactions with all other interfaces in the stratification. This is done for efficiency, though it is justified physically for most practical applications, but it is no fundamental limitation, since the full Green's function formulation in Eq. (8)-(9) may be used also locally.

## Numerical Issues

The efficiency of the virtual source approach hinges on a number of numerical issues, primarily associated with the details of the distribution of surface nodes and virtual sources, but also the implementation of the spectral integral representations of the waveguide Green's function.

*Virtual Source Distribution.* Work is ongoing in terms of developing a systematic, adaptive approach to the distribution of the virtual sources inside the targets. However, it has been found empirically that a consistent convergence is achieved by distributing the surface nodes with a separation which is proportional to the local radii of curvature, and by placing a virtual source along the inward normal at each node, at a depth of approximately 0.6 times the node separation. This seems to provide the optimal compromise between diagonal dominance of the matrix to be inverted in Eq. (6) and efficient use of the dynamic range.

*Fourier-Bessel Green's Function Representation.* The computationally most intensive component of the present approach is the evaluation of the  $N \times N$  pressure and displacement Green's function matrices  $\mathbf{P}$  and  $\mathbf{U}$  in Eq. (6) through the Fourier-Bessel representations in Eqs. (8)-(9). Here it is extremely important to take advantage of any target symmetries. Thus for example, for targets with vertical axisymmetry, the virtual sources and surface nodes are naturally placed in 'rings' at constant depth, thus reducing the number of required values of the depth-separated Green's function. Also, this will reduce the number of required values of the Bessel functions. In that regard, the fact that the Green's functions are only needed in the near field with  $k_r r$  small, makes it convenient to pre-compute a table of Bessel functions with  $\Delta k_r r \simeq \pi/20$  from which the required values are extracted by simple interpolation. Further, the wavenumber integration interval may be reduced significantly by replacing Eq. (8) with the exact free field Green's function  $\exp(jkR)/4\pi R$  for all source-receiver pairs in the same layer.

Finally, for computing the scattered field, significant computational gains are achieved by performing the inner summation in Eq. (8) for a reference depth, e.g.  $z_i$ , within each layer before solving for the homogeneous solution in Eq. (9), essentially collapsing the virtual source distribution into a multipole at  $(r, z) = (0, z_i)$ . It should be pointed out that this procedure yields incorrect field solution within the depth-interval occupied by the target due to incorrect representation of the evanescent contribution. However, as long as the field is not needed at these depths, it yields significant computational savings.

## NUMERICAL RESULTS

### Spherical Shell in Free Space

The first example concerns the free field scattering of a plane wave incident on a spherical, elastic shell in an infinite medium. The sphere considered is the 1.06 m outer diameter air-filled steel sphere used as a target in the GOATS experiments, and

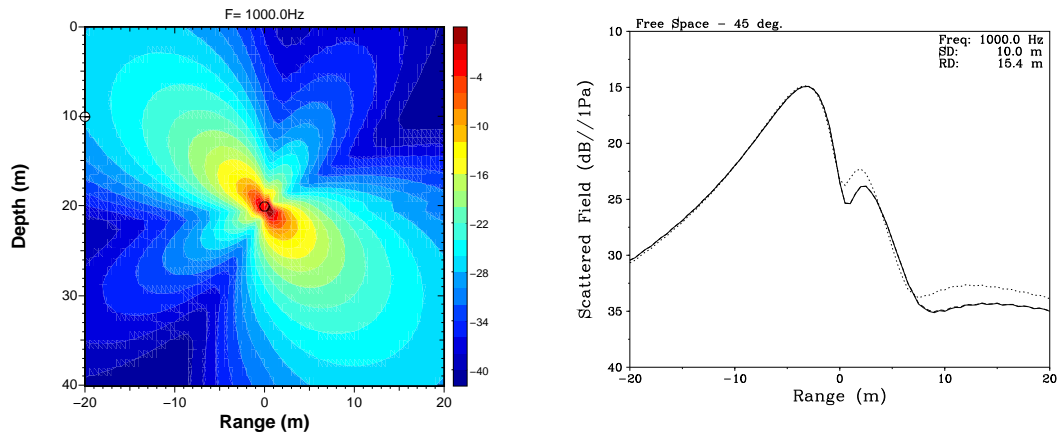


**FIGURE 2.** In-plane scattered field for spherical shell in a homogeneous fluid medium insonified by a unit amplitude plane wave incident at  $45^\circ$ . a) Contours of scattered pressure in dB in vertical plane. Spherical target at origin as indicated. (b) Scattered pressure 4.6 m above target center in dB Solid curve: Reference solution using spherical harmonics; Dashed curve: Virtual source solution with 1146 nodes; Dotted curve: Virtual source solution with 732 nodes.

extensively analyzed in terms of its scattering characteristics [10]. The shell thickness is 3 cm and the sound speed in the surrounding fluid is assumed to be 1500 m/s.

Figure 2(a) shows contours in dB of the in-plane scattered field for a 1 kHz plane wave incident at  $45^\circ$ , as computed using an exact multipole expansion obtained by spherical harmonics, but with the field evaluated using the Fourier-Bessel spectral representation in Eq. (8). Note the small errors at the depth of the target due to the point-multipole representation of the vertically extended target as discussed above. Figure 2(b) shows the scattered field in negative dB along a horizontal line 4.6 m above the target. The solid curve shows the spherical harmonics solution, while the dotted curve shows the result obtained by the virtual source approach using 732 virtual sources (24 horizontal rings). Almost indistinguishable from the 'exact' spherical harmonics result, a dashed curve shows the virtual source result obtained with 1146 sources (30 rings). The target stiffness matrix was in both cases computed using both spherical harmonics, and FESTA, with virtually identical results.

In the absence of interfaces penetrating the target both virtual source results in Fig.2 were obtained using the exact free field Green's functions in Eq. (6).

To illustrate the accuracy of the Fourier-Bessel spectral representation of the Green's function, Fig. 3 compares the in-plane scattered field 1m from the target center, using the Fourier-Bessel representation with a dummy interface at the depth of the target center (solid curve), with the field obtained using the exact spherical Green's function for the same virtual source distribution (dashed curve).

## Flush-buried Spherical Shell

The final example demonstrates the significance of properly incorporating multiple scattering when modeling the response of targets close to the interfaces in the stratifi -

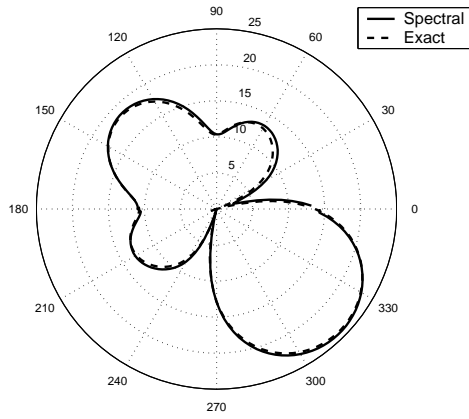


**FIGURE 3.** In-plane scattered field from spherical shell in infinite, homogeneous medium, 1 m from target center, using multipole, spectral representation of Green’s functions (solid curve) and free field exact spherical Green’s function  $exp(ikR)/R$  (dashed curve)

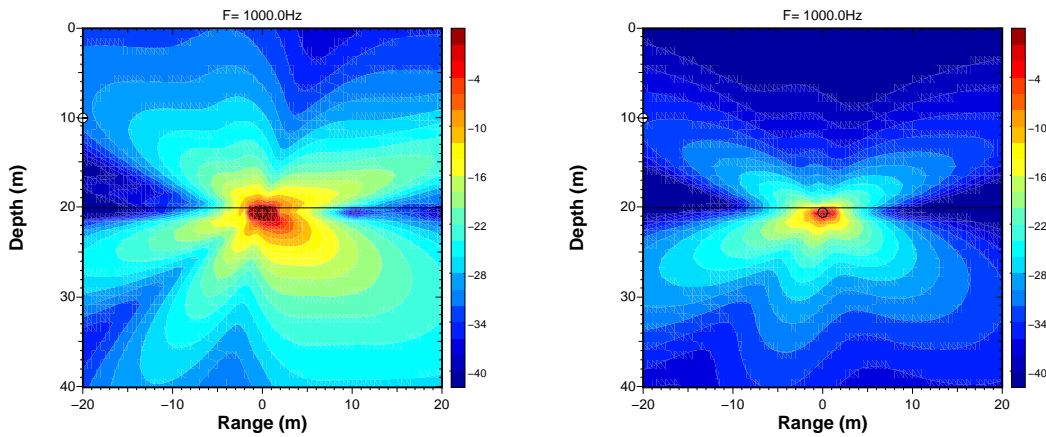


**FIGURE 4.** Pressure contours in dB of in-plane scattering from flush-buried spherical shell for plane wave incident at  $10^\circ$  grazing onto seabed. (a) Multiple scattering included using spectral representation of dual-halfspace Green’s function. (b) Single scatterer approximation using free field Green’s function for virtual source contributions.

cation. Here the spherical shell treated above is assumed to be flush-buried in a seabed with sound speed 1700 m/s and density  $1.8 \text{ g/cm}^3$ , and insonified by a 1 kHz plane wave from the water column, at sub-critical  $10^\circ$  grazing angle, thus yielding an evanescent incident field in the seabed. The 1146 node target stiffness matrix of the previous example is used here unchanged. Figure 4(a) shows the in-plane pressure contours in dB using the Fourier-Bessel integral representation of the Green’s functions in Eq. (6), while (b) shows the corresponding result using the free-field Green’s functions for the sediment. In both cases the resulting scattered field is evaluated using the full stratified Green’s function, and the significant difference observed in the scattered field illustrates the importance of incorporating multiple scattering for these problems. In contrast Fawcett [11] found single scattering to be adequate, but for deeper buried targets.

## SUMMARY

A hybrid modeling framework for scattering from general 3D elastic targets in a stratified ocean waveguide has been presented, incorporating multiple scattering between the target and the stratification, and allowing for targets to be completely or partially buried in an elastic seabed. The main components of the hybrid framework are (i) a stiffness matrix uniquely describing the dynamic properties of the target in vacuo, (ii) the spectral Fourier-Bessel representation of the Green's function in a horizontally stratified ocean. The two components are coupled through a wavefield superposition, or virtual source approach, where the scattered field on the surface of the target is 'generated' by a distribution of virtual sources inside the volume occupied by the target, and which superimposed with the incident field must be consistent with the surface stiffness properties of the target. The hybrid approach is here implemented within the OASES-3D wavenumber integration modeling framework, with the target response determined using spherical harmonics [12] for spherical shells, or FESTA [5] for more general targets.

## ACKNOWLEDGMENTS

The author appreciates the collaboration with Dr. Mario Zampolli and David Burnett of SACLANTCEN on the integration of FESTA and OASES. The SACLANTCEN support of the collaborate modeling effort through the GOATS and the Hybrid Modeling JRP is highly appreciated, as is the support by the US Office of Naval Research.

## REFERENCES

1. Schmidt, H., and Lee, J., *J. Acoust. Soc. Am.*, **105**, 1605–1617 (1999).
2. Maguer, A., Fox, W., Schmidt, H., Pouliquen, E., and Bovio, E., *J. Acoust. Soc. Am.*, **107**(3), 1215–1225 (2000).
3. Schmidt, H., “Bistatic scattering from buried targets in shallow water,” in *Proceedings, GOATS 2000 Conference*, edited by E. Bovio and H. Schmidt, SACLANTCEN Conference Proceedings Series CP-46, NATO SACLANT Undersea Research Centre, La Spezia, Italy, 2001.
4. Schmidt, H., and Glattetre, J., *J. Acoust. Soc. Am.*, **78**, 2105–2114 (1985).
5. Burnett, D., and Zampolli, M., Development of a steady-state, 3-d acoustics code for target scattering, SR 379, NATO Undersea Research Centre, La Spezia, Italy (2003).
6. Burnett, D., “Finite-element methods for structural acoustics: physics, mathematics and modeling,” in *Proceedings, 10th Internat. Congress on Sound and Vibration*, Stockholm, Sweden, 2003.
7. Stepanishen, P., *J. Acoust. Soc. Am.*, **101**, 3270–3277 (1997).
8. Kessel, R. T., *Scattering of elastic waves in layered media: a boundary integral-normal mode method*, Ph.D. thesis, University of Victoria (1996).
9. Jensen, F., Kuperman, W., Porter, M., and Schmidt, H., *Computational Ocean Acoustics*, AIP Press, New York, 1994.
10. Tesei, A., Lim, R., Maguer, A., Fox, W., and Schmidt, H., *J. Acoust. Soc. Am.*, **112**(5), 1817–1830 (2002).
11. Fawcett, J., “Scattering from an elastic cylinder buried beneath a rough water/basement interface,” in *High Frequency Acoustics in Shallow Water*, edited by N. Pace, E. Pouliquen, O. Bergem, and A. Lyons, SACLANTCEN Conference proceedings Series CP-45, 1997.
12. Schmidt, H., *J. Acoust. Soc. Am.*, **94**(4), 2420–2430 (1993).